Electronic Supplementary Material (ESI) for Lab on a Chip.

Supplementary Information

Tumor antigen-independent and cell size variation-inclusive enrichment of viable circulating tumor cells

Wujun Zhao,[ab] Yang Liu,[a] Brittany D. Jenkins,[c] Rui Cheng,[b] Bryana N. Harris,[d] Weizhong Zhang,[a] Jin Xie,[a] Jonathan R. Murrow,[e] Jamie Hodgson,[f] Mary Egan,[f] Ana Bankey,[f] Petros G. Nikolinakos,[f] Haythem Y. Ali,[g] Kristina Meichner,[h] Lisa A. Newman,[ij] Melissa B. Davis,*[cjk] and Leidong Mao*[b]

[a]Department of Chemistry, The University of Georgia, Athens, GA 30602, USA

[b]School of Electrical and Computer Engineering, The University of Georgia, Athens, GA 30602, USA

[c]Department of Genetics, The University of Georgia, Athens, GA 30602, USA

[d]Department of Chemical Engineering, Auburn University, Auburn, AL 36830, USA

[e]Department of Medicine, Augusta University-The University of Georgia Medical Partnership, Athens, GA 30602, USA

[f]University Cancer & Blood Center, LLC, Athens, GA, 30607

[g]Department of Hematology and Oncology, Henry Ford Health System, Detroit, MI 48202, USA

[h]Department of Pathology, College of Veterinary Medicine, The University of Georgia, Athens, GA 30602, USA

[i]Department of Surgery, Henry Ford Health System, Detroit, MI 48202, USA

[j]Department of Surgery, Weill Cornell Medicine, New York, NY 10021

[k]Department of Public Health Sciences, Henry Ford Health System and Henry Ford Cancer Institute, Detroit, MI 48202, USA

These authors contributed equally: Wujun Zhao and Yang Liu

*Emails: Leidong Mao (mao@uga.edu) and Melissa B. Davis (mbd4001@med.cornell.edu)

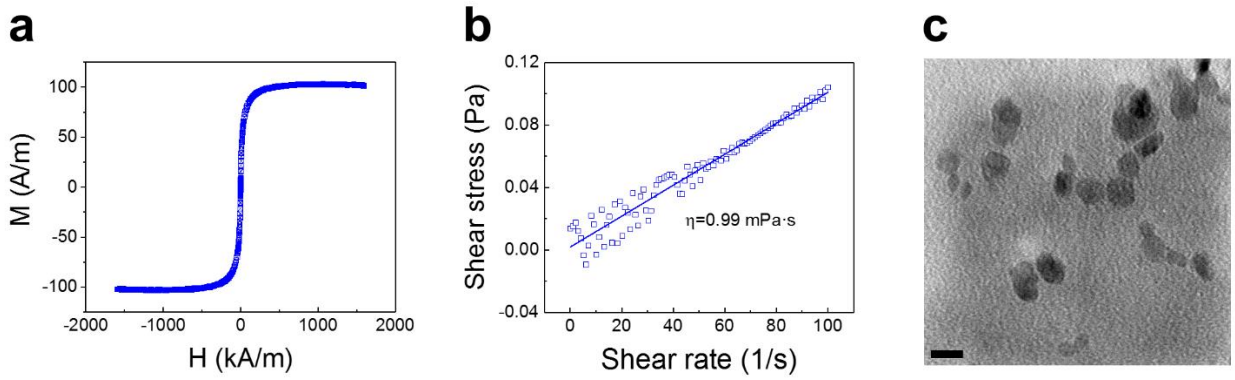

Fig. 1 a Magnetization of the as-synthesized ferrofluid. Saturation magnetization of this ferrofluid was 0.104 kA m^{-1}, corresponding to a 0.028% volume fraction or concentration. **b** Rheological plot of the ferrofluid. The viscosity of ferrofluid was measured to be 0.99 mPa·s. **c** A transmission electron microscopy (TEM) image of the maghemite nanoparticles. Scale bar: 10 nm.

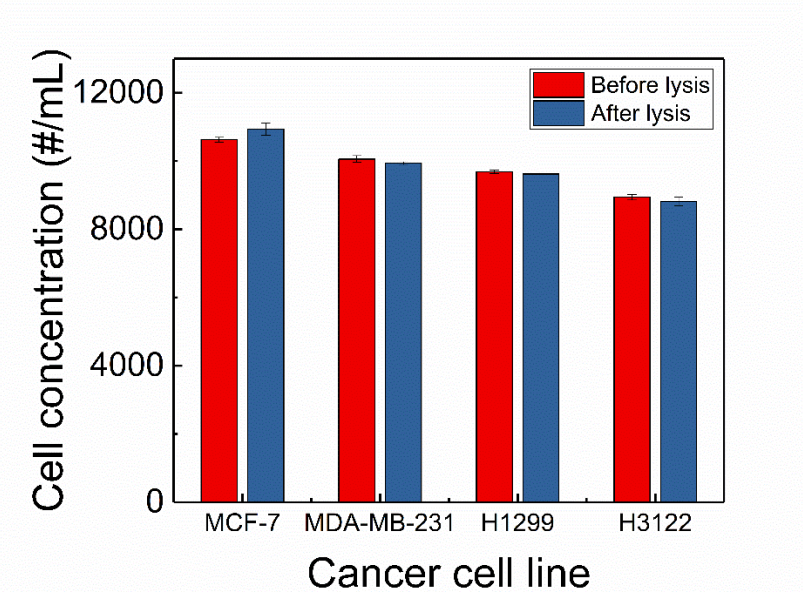

Fig. 2 RBC lysis effect on cancer cells. ~10,000 cancer cells were spiked into 1 mL of media. The number of cancer cells were counted twice in a Nageotte counting chamber. Lysis buffer and centrifugation step were carried out exactly as the protocol in processing patient samples. Cancer cells pellet were then resuspended in 1 mL of media and counted twice. Same experiments were repeated for 4 cancer cell lines (MCF-7, MDA-MB-231, H1299 and H3122). We used recovery rate, defined as the number of cells after lysis and centrifugation over the number of cells before lysis and centrifugation, to represent the cell loss. Data on 4 cells lines are: MCF-9 recovery rate 102.92%, MDA-MB-231 recovery rate 98.81%, H1299 recovery rate 99.28%, and H3122 recovery rate 98.66%. Mean cell loss after lysis and centrifugation across 4 cancer cell lines is 0.08%. Error bars are standard deviation (n=2).

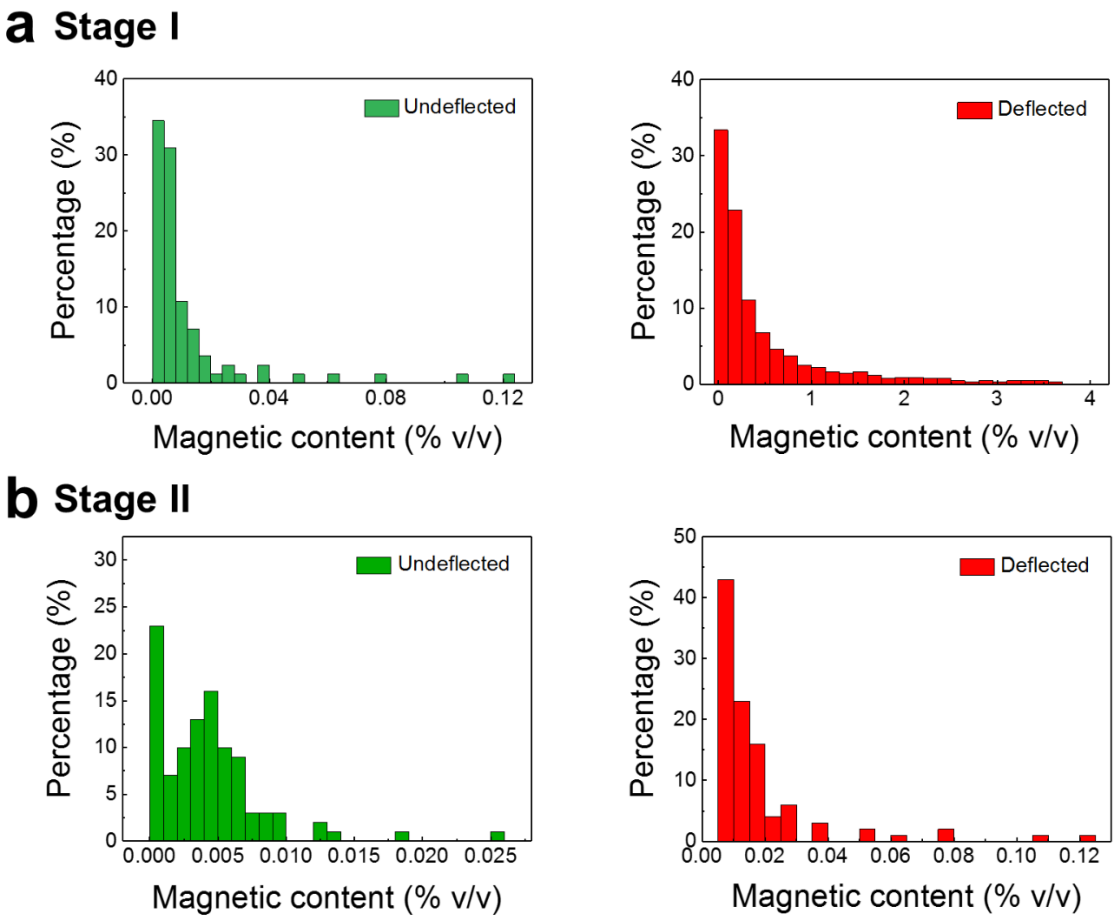

Fig. 3 a Magnetic content of undeflected and deflected white blood cells (WBCs) at stage I. **b** Magnetic content of undeflected and deflected WBCs at stage II.

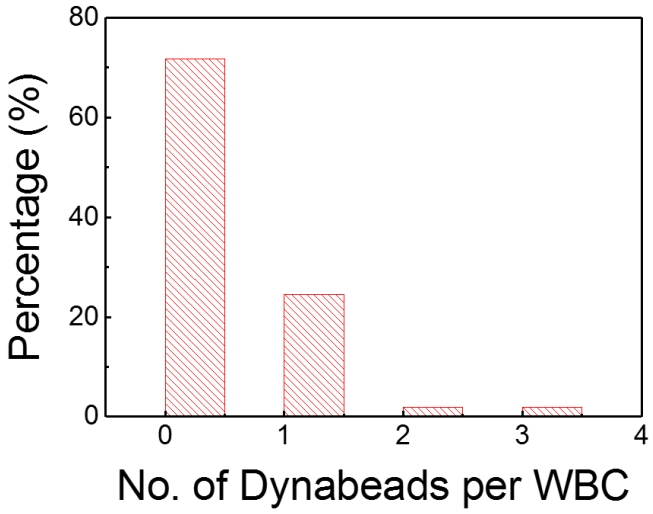

Fig. 4 Number of Dynabeads per white blood cell (WBC) after cell enrichment. The device carried over on average 533±34 WBCs per 1 milliliter of blood processed. Much of the carryover was derived from WBCs that were either not labeled or labeled with just one magnetic bead.

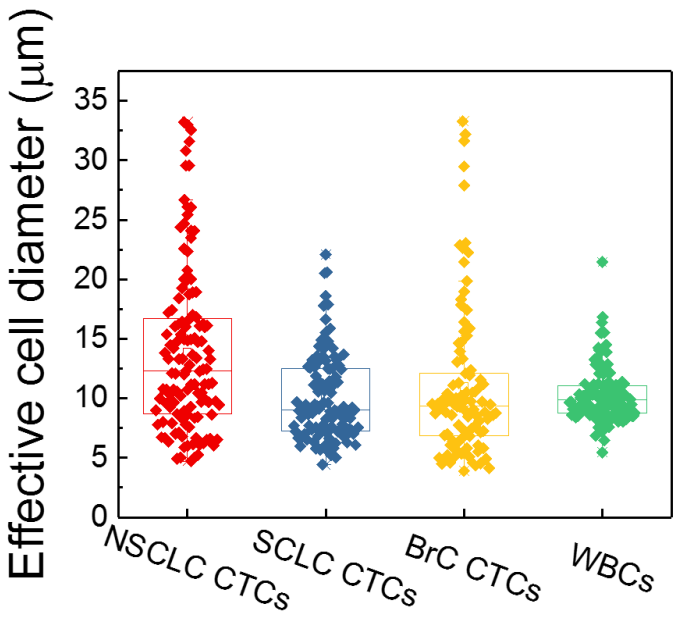

Fig. 5 Size distribution of clinical CTCs from non-small cell lung cancer (NSCLC) patients, small cell lung cancer (SCLC) patients, and breast cancer (BrC) patients. Details are listed in Supplementary Tab. 5.

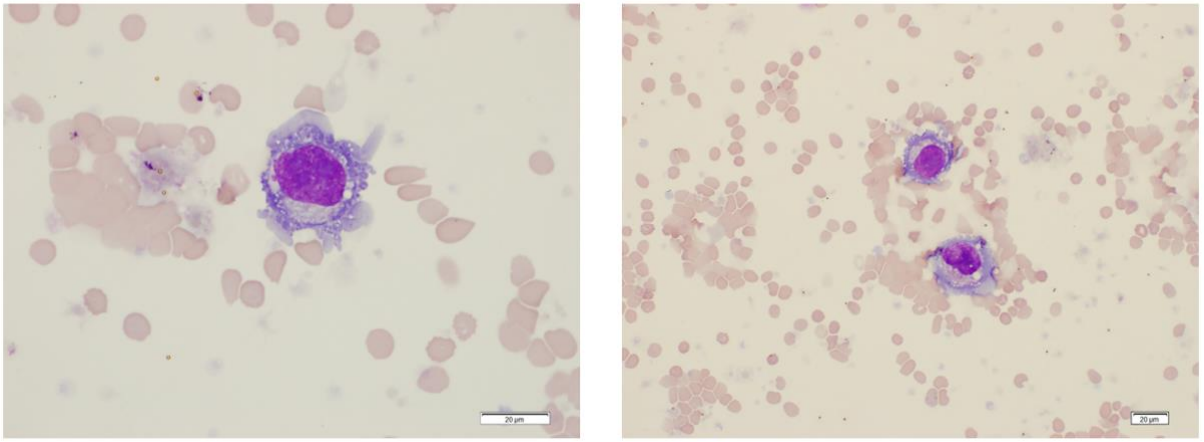

Fig. 6 Cytopathological staining of spiked HCC1806 cancer cells after enrichment. Scale bars: 20 μm.

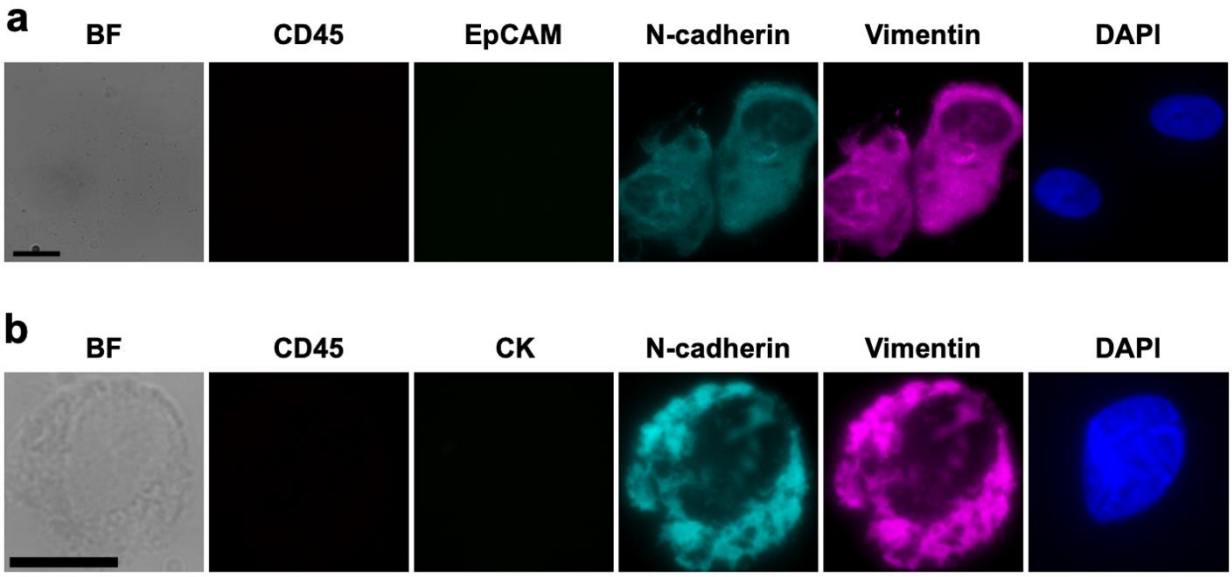

Fig. 7 a Bright field and immunofluorescent images of CTCs enriched from breast cancer patient. Five channels were used in immunofluorescent staining, including leukocyte marker CD45 (red), epithelial CTC marker EpCAM (green), mesenchymal CTC markers N-cadherin (N-cad, cyan) and vimentin (Vim, magenta), and nucleus marker DAPI (blue). **b** Bright field and immunofluorescent images of CTC enriched from lung cancer patients. Five channels were used in immunofluorescent staining, including leukocyte marker CD45 (red), epithelial CTC marker CK (green), mesenchymal CTC markers N-cadherin (N-cad, cyan) and vimentin (Vim, magenta), and nucleus marker DAPI (blue). Scale bars: 10 μm.

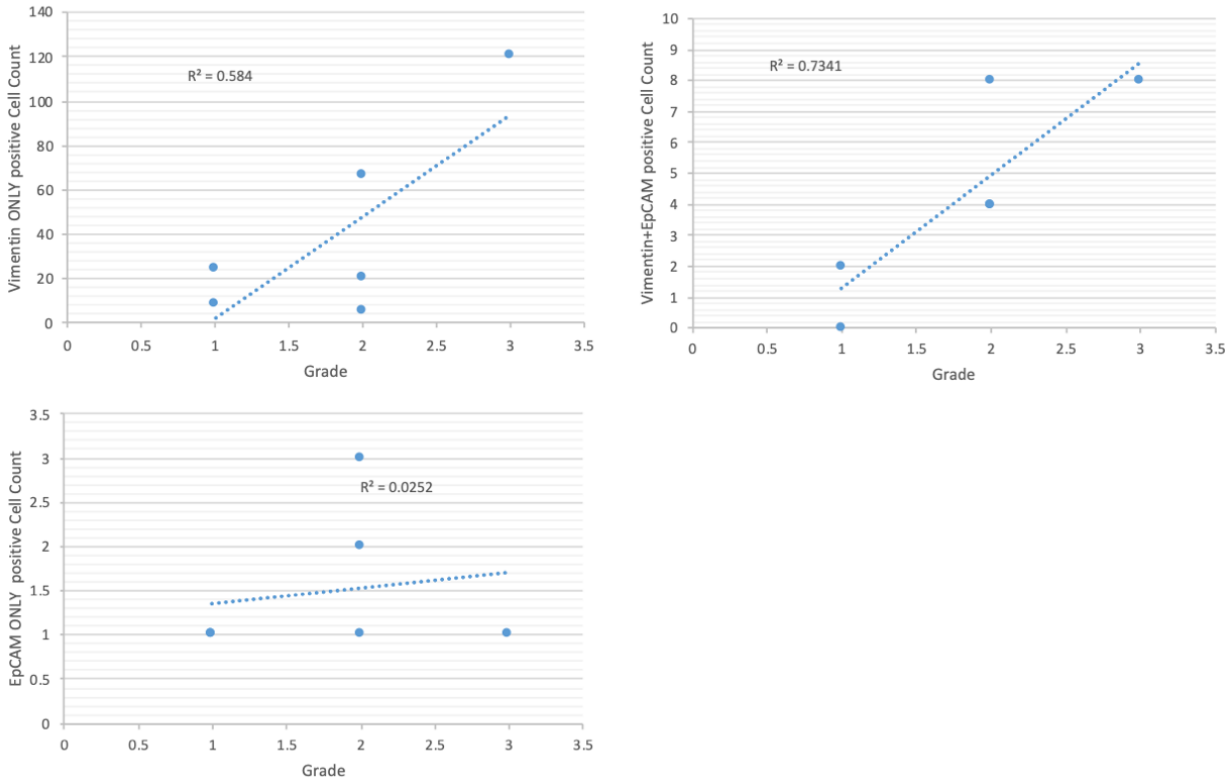

Fig. 8 Correlation of the numbers of each CTC subtype with tumor grade in third cancer patient cohort.

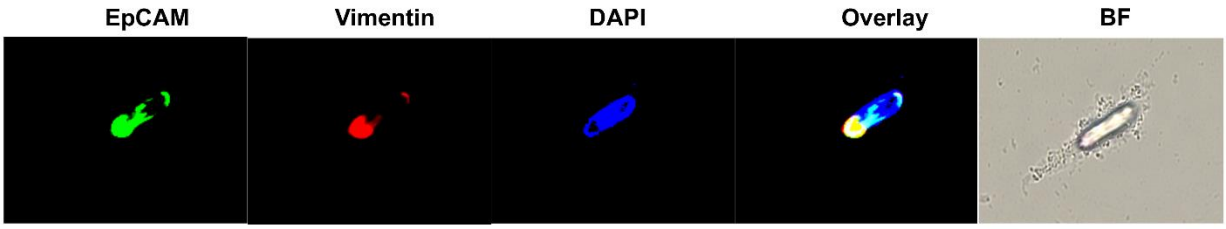

Fig. 9 Bright field and immunofluorescent images of a representative cell from CTC culture of BrC-P2-Culture. Cells were subjected to multiplexed immunofluorescence assessment with cell-type specific markers detected with distinct channels, including epithelial CTC marker EpCAM (green), mesenchymal CTC marker vimentin (red), and DAPI (blue).

Tab. 1 Clinical information of cancer patients and CTC enumeration from each patient.

Sample Number	Tumor type	Stage	Volume (mL)	CTC enumeration
BrC-P1-Culture	BrC	IA	9.5	20
BrC-P2-Culture	BrC	IB	8.9	5
BrC-P3-Culture	BrC	IA	8.8	8
BrC-P4-Culture	BrC	IIA	8.5	120
BrC-P5-Culture	BrC	IA	7.5	66
BrC-P6-Culture	BrC	IA	5.7	24
BrC-P1-Optimization	BrC	IIIA	9.0	232
BrC-P2-Optimization	BrC	IA	12.0	82
BrC-P3-Optimization	BrC	IA	3.0	63
LC-P1-Optimization	NSCLC	IV	9.0	228
LC-P2-Optimization	SCLC	IV	9.0	202
LC-P3-Optimization	SCLC	IV	9.0	222

Tab. 2 A survey of existing CTC enrichment methods.

Type	Technique	Size-based/ antigen-based?	Throughput (mL/h)	Recovery rate	Purity	Viability	Reference
Immunoaffinity	CellSearch	Antigen	N/A	~81%	N/A	N/A	[1]
	Magsweeper	Antigen	9	59±27%	~100%	N/A	[2]
Microfluidic micropost	CTC-Chip	Antigen	1	>60%	~ 56%	98.5%	[3]
	GEDI	Antigen	1	~85%	~68%	N/A	[4]
	OncoCEE	Antigen	1	~80-90%	N/A	N/A	[5]
	NanoVelcro-Chip	Antigen	0.5	~90%	N/A	N/A	[6]
Microfluidic surface capture	HB-Chip	Antigen	1.2	~91.8%	14%	95%	[7]
	GEM-Chip	Antigen	3.6	~90%	~84%	~85%	[8]
	Graphene Oxide Chip	Antigen	~1-3	73±2.4%	N/A	N/A	[9]
Immunomagnetic positive	Ephesia-Chip	Antigen	3	~90%	<100 contaminating cells	N/A	[10]
	Magnetic Sifter	Antigen	10	~90% for high EpCAM expressing cells; < 48% for low EpCAM expressing cells	17.7±9.3%	N/A	[11]
	Isoflux	Antigen	1.2	74-85%	~1.4 %	N/A	[12]
	CTC-iChip	Antigen&Size	8	89.7-98.6%	> 0.1 %	N/A	[13]
	Micromagnetic Chip	Antigen	1.2	~90 %	remove > 99.6% WBC	>90%	[14]
	IMN	Antigen	1.2	~94%	N/A	93%	[15]
	MAP (magnetophoresis)	Antigen	10	86-90%	N/A	N/A	[16]
Immunomagnetic negative	QMS	Antigen	1-10 million cells per second	46%	~0.1 - 6.4%	~90%	[17]
	EasySep™ Human CD45 Depletion Kit	Antigen	N/A	69%	1%	N/A	[18]
	CTC-iChip	Antigen	8	~ 97%	~7.8%	N/A	[13]
	Monolithic CTC-iChip	Antigen	15-20 million cells per second	~99.5%	18.4% (445 WBCs per mL)	N/A	[19]
Density gradient centrifugation	Ficoll-Paque	Density	20	N/A	N/A	N/A	[20]
	OncoQuick	Density	N/A	N/A	N/A	N/A	[21]
Density-antibody	RosetteSep™ CTC Enrichment Cocktail	Antigen&Density	N/A	~62.5%	N/A	N/A	[22]
	Accucyte Enrichment and CyteSealer™	Antigen&Density	N/A	~90.5%	N/A	N/A	[23]

Size-deformability	ISET®	Size	N/A	N/A	N/A	N/A	[24]
	ScreenCell®	Size	1 mL/min	74-91.2%	N/A	~85%	[25]
	CellSieve	Size	2.5. mL/min	N/A	N/A	N/A	[26]
	FMSA	Size	0.75 mL/min	90%	Remove 99.99% WBCs	80%	[27]
	SB microfilter	Size	N/A	78-83%	Remove ~99.95% WBCs	71-74%	[28]
	RCT (Resettable Cell Trap)	Size	0.6	>90%	Remove ~99.89% WBCs	N/A	[29]
	Cluster Chip	Size	2.5	41-99%	~15%	~95%	[30]
Inertial focusing	Vortex	Size	22.5	21%	57-94%	~86%	[31]
	DFF (Dean Flow Fractionation)	Size	3	>85%	Remove ~ 99.95% WBCs	> 98%	[32]
Electrophoresis	ApoStream™	DEP	~1.3	~73%	Remove ~99.99% peripheral blood mononuclear cells (PBMCs)	97.1%	[33]
Acoustophoresis	taSSAW-Chip	Size	1.2	~83%	Remove >90% WBCs	~91%	[34]
	Acoustophoresis Chip	Size	6	~95%	~97.8	N/A	[35]
Magnetophoresis	FCS	Size	6	~92.9%	11.7%	96.3%	[36]
	iFCS (this manuscript)	Size variation-inclusive (down to 3 µm)	12	99.16%	533 WBCs per mL blood	97.69%	N/A

Tab. 3 Cell size distribution (maximum ferret diameter) of cancer cell lines and WBCs. Date are expressed as mean ± standard deviation (s.d.) in the last column.

Cell line	Cancer cell type	Measured minimum diameter (μm)	Measured Average diameter (μm)
PC-3	Prostate	6.64	19.89±4.64
MCF7	Breast	6.99	17.48±4.28
HCC1806	Breast	6.65	15.42±2.35
MDA-MB-231	Breast	6.96	19.10±3.56
H1299	NSCLC	7.22	20.41±3.39
H3122	NSCLC	6.46	21.34±6.08
H69	SCLC	3.86	11.20±3.51
DMS79	SCLC	3.22	12.80±5.87
WBC	N/A	6.68	11.06±2.08

Tab. 4 Cell diameter (maximum ferret diameter) distribution of spiked and recovered cancer cells undergoing an iFCS process. Data are expressed as mean ± standard deviation (s.d.) in the last two columns.

Cell line	Minimum diameter (spiked, µm)	Minimum diameter (recovered, µm)	Average diameter (spiked, µm)	Average diameter (recovered, µm)
MCF7	6.99	6.64	17.48±4.28	18.76±5.31
MDA-MB-231	6.96	6.97	19.10±3.57	19.92±4.59
PC-3	8.07	6.64	19.89±4.64	20.44±4.86

Tab. 5 Size distribution (maximum ferret diameter) of clinical CTCs from non-small cell lung cancer (NSCLC), small cell lung cancer (SCLC), and breast cancer (BrC) patients.

Cell diameter	<6 µm	6-8 µm	8-10 µm	10-15 µm	>15 µm	Mean±s.d. (µm)	Minimum (µm)	Median (µm)	Maximum (µm)
NSCLC CTCs (n=166)	7.8%	25.3%	16.9%	24.1%	25.9%	12.28±6.62	4.71	10.09	33.23
SCLC CTCs (n=110)	9.1%	27.3%	24.5%	30.9%	8.2%	10.00±3.67	4.41	8.99	22.08
BrC CTCs (n=101)	19.8%	14.8%	23.8%	22.8%	18.8%	10.99±6.46	3.89	9.37	33.29
WBCs (n=134)	0.7%	9.0%	41.8%	44.0%	4.5%	10.25±2.30	5.48	9.88	21.45

Tab. 6 Comparison of design, operation and CTC enrichment performances between CTC-iChip and iFCS.

Technology	Blood processing throughput (mL h^{-1})	CTC recovery rate (spiked cell lines)	White blood cells (WBC) carryover at device outlet	Recovered CTC diameter range	Cell viability (cell lines)	Design and operation	Red blood cell lysis needed?
CTC-iChip[13]	8	~ 97%	32,000 WBCs/mL	>9 μm	Not reported	Integration of DLD, inertial focusing and magnetophoresis in two devices. Separate optimization needed.	No
Monolithic CTC-iChip[19]	~10	~99.5%	445 WBCs/mL	5.5-27 μm	Not reported	Integration of DLD, inertial focusing and magnetophoresis in a single device. Separate optimization needed.	No
iFCS	12	99.08%	533 WBCs/mL	>3 μm	97.69%	Integration of diamagnetophoresis / magnetophoresis in a single device. A single physical model for optimization.	Yes

References

1. S. Riethdorf, H. Fritsche, V. Muller, T. Rau, C. Schindibeck, B. Rack, W. Janni, C. Coith, K. Beck, F. Janicke, S. Jackson, T. Gornet, M. Cristofanilli and K. Pantel, *Clin Cancer Res*, 2007, **13**, 920-928.

2. A. H. Talasaz, A. A. Powell, D. E. Huber, J. G. Berbee, K. H. Roh, W. Yu, W. Z. Xiao, M. M. Davis, R. F. Pease, M. N. Mindrinos, S. S. Jeffrey and R. W. Davis, *Proceedings of the National Academy of Sciences of the United States of America*, 2009, **106**, 3970-3975.

3. S. Nagrath, L. V. Sequist, S. Maheswaran, D. W. Bell, D. Irimia, L. Ulkus, M. R. Smith, E. L. Kwak, S. Digumarthy, A. Muzikansky, P. Ryan, U. J. Balis, R. G. Tompkins, D. A. Haber and M. Toner, *Nature*, 2007, **450**, 1235-U1210.

4. J. P. Gleghorn, E. D. Pratt, D. Denning, H. Liu, N. H. Bander, S. T. Tagawa, D. M. Nanus, P. A. Giannakakou and B. J. Kirby, *Lab Chip*, 2010, **10**, 27-29.

5. S. D. Mikolajczyk, L. S. Millar, P. Tsinberg, S. M. Coutts, M. Zomorrodi, T. Pham, F. Z. Bischoff and T. J. Pircher, *Journal of Oncology*, 2011, DOI: Artn 25236110.1155/2011/252361.

6. Y. T. Lu, L. B. Zhao, Q. L. Shen, M. A. Garcia, D. X. Wu, S. Hou, M. Song, X. C. Xu, W. H. OuYang, W. W. L. OuYang, J. Lichterman, Z. Luo, X. Xuan, J. T. Huang, L. W. K. Chung, M. Rettig, H. R. Tseng, C. Shao and E. M. Posadas, *Methods*, 2013, **64**, 144-152.

7. S. L. Stott, C. H. Hsu, D. I. Tsukrov, M. Yu, D. T. Miyamoto, B. A. Waltman, S. M. Rothenberg, A. M. Shah, M. E. Smas, G. K. Korir, F. P. Floyd, A. J. Gilman, J. B. Lord, D. Winokur, S. Springer, D. Irimia, S. Nagrath, L. V. Sequist, R. J. Lee, K. J. Isselbacher, S. Maheswaran, D. A. Haber and M. Toner, *Proceedings of the National Academy of Sciences of the United States of America*, 2010, **107**, 18392-18397.

8. W. A. Sheng, O. O. Ogunwobi, T. Chen, J. L. Zhang, T. J. George, C. Liu and Z. H. Fan, *Lab Chip*, 2014, **14**, 89-98.

9. H. J. Yoon, T. H. Kim, Z. Zhang, E. Azizi, T. M. Pham, C. Paoletti, J. Lin, N. Ramnath, M. S. Wicha, D. F. Hayes, D. M. Simeone and S. Nagrath, *Nature nanotechnology*, 2013, **8**.

10. J. Autebert, B. Coudert, J. Champ, L. Saias, E. T. Guneri, R. Lebofsky, F. C. Bidard, J. Y. Pierga, F. Farace, S. Descroix, L. Malaquin and J. L. Viovy, *Lab Chip*, 2015, **15**, 2090-2101.

11. C. M. Earhart, C. E. Hughes, R. S. Gaster, C. C. Ooi, R. J. Wilson, L. Y. Zhou, E. W. Humke, L. Y. Xu, D. J. Wong, S. B. Willingham, E. J. Schwartz, I. L. Weissman, S. S. Jeffrey, J. W. Neal, R. Rohatgi, H. A. Wakeleebe and S. X. Wang, *Lab Chip*, 2014, **14**, 78-88.

12. W. Harb, A. Fan, T. Tran, D. C. Danila, D. Keys, M. Schwartz and C. Ionescu-Zanetti, *Transl Oncol*, 2013, **6**, 528-+.

13. E. Ozkumur, A. M. Shah, J. C. Ciciliano, B. L. Emmink, D. T. Miyamoto, E. Brachtel, M. Yu, P. I. Chen, B. Morgan, J. Trautwein, A. Kimura, S. Sengupta, S. L. Stott, N. M. Karabacak, T. A. Barber, J. R. Walsh, K. Smith, P. S. Spuhler, J. P. Sullivan, R. J. Lee, D. T. Ting, X. Luo, A. T. Shaw, A. Bardia, L. V. Sequist, D. N. Louis, S. Maheswaran, R. Kapur, D. A. Haber and M. Toner, *Sci Transl Med*, 2013, **5**.

14. J. H. Kang, S. Krause, H. Tobin, A. Mammoto, M. Kanapathipillai and D. E. Ingber, *Lab Chip*, 2012, **12**, 2175-2181.

15. M. Tang, C. Y. Wen, L. L. Wu, S. L. Hong, J. Hu, C. M. Xu, D. W. Pang and Z. L. Zhang, *Lab Chip*, 2016, **16**, 1214-1223.

16. K. Hoshino, Y. Y. Huang, N. Lane, M. Huebschman, J. W. Uhr, E. P. Frenkel and X. J. Zhang, *Lab Chip*, 2011, **11**, 3449-3457.

17. O. Lara, X. D. Tong, M. Zborowski and J. J. Chalmers, *Exp Hematol*, 2004, **32**, 891-904.

18. Z. A. Liu, A. Fusi, E. Klopocki, A. Schmittel, I. Tinhofer, A. Nonnenmacher and U. Keilholz, *J Transl Med*, 2011, **9**.

19. F. Fachin, P. Spuhler, J. M. Martel-Foley, J. F. Edd, T. A. Barber, J. Walsh, M. Karabacak, V. Pai, M. Yu, K. Smith, H. Hwang, J. Yang, S. Shah, R. Yarmush, L. V. Sequist, S. L. Stott, S. Maheswaran, D. A. Haber, R. Kapur and M. Toner, *Sci Rep-Uk*, 2017, **7**.

20. J. Weitz, P. Kienle, J. Lacroix, F. Willeke, A. Benner, T. Lehnert, C. Herfarth and M. von Knebel Doeberitz, *Clin Cancer Res*, 1998, **4**, 343-348.

21. G. A. Clawson, E. Kimchi, S. D. Patrick, P. Xin, R. Harouaka, S. Zheng, A. Berg, T. Schell, K. F. Staveley-O'Carroll, R. I. Neves, P. J. Mosca and D. Thiboutot, *PLoS One*, 2012, **7**, e41052.

22. W. He, S. A. Kularatne, K. R. Kalli, F. G. Prendergast, R. J. Amato, G. G. Klee, L. C. Hartmann and P. S. Low, *Int J Cancer*, 2008, **123**, 1968-1973.

23. D. E. Campton, A. B. Ramirez, J. J. Nordberg, N. Drovetto, A. C. Clein, P. Varshavskaya, B. H. Friemel, S. Quarre, A. Breman, M. Dorschner, S. Blau, C. A. Blau, D. E. Sabath, J. L. Stilwell and E. P. Kaldjian, *BMC Cancer*, 2015, **15**, 360.

24. G. Vona, A. Sabile, M. Louha, V. Sitruk, S. Romana, K. Schutze, F. Capron, D. Franco, M. Pazzagli, M. Vekemans, B. Lacour, C. Brechot and P. Paterlini-Brechot, *Am J Pathol*, 2000, **156**, 57-63.

25. I. Desitter, B. S. Guerrouahen, N. Benali-Furet, J. Wechsler, P. A. Janne, Y. Kuang, M. Yanagita, L. Wang, J. A. Berkowitz, R. J. Distel and Y. E. Cayre, *Anticancer Res*, 2011, **31**, 427-441.

26. D. L. Adams, S. S. Martin, R. K. Alpaugh, M. Charpentier, S. Tsai, R. C. Bergan, I. M. Ogden, W. Catalona, S. Chumsri, C.-M. Tang and M. Cristofanilli, 2014, DOI: 10.1073/pnas.1320198111 %J Proceedings of the National Academy of Sciences, 201320198.

27. R. A. Harouaka, M. D. Zhou, Y. T. Yeh, W. J. Khan, A. Das, X. Liu, C. C. Christ, D. T. Dicker, T. S. Baney, J. T. Kaifi, C. P. Belani, C. I. Truica, W. S. El-Deiry, J. P. Allerton and S. Y. Zheng, *Clin Chem*, 2014, **60**, 323-333.

28. M. D. Zhou, S. Hao, A. J. Williams, R. A. Harouaka, B. Schrand, S. Rawal, Z. Ao, R. Brenneman, E. Gilboa, B. Lu, S. Wang, J. Zhu, R. Datar, R. Cote, Y. C. Tai and S. Y. Zheng, *Sci Rep*, 2014, **4**, 7392.

29. X. Qin, S. Park, S. P. Duffy, K. Matthews, R. R. Ang, T. Todenhofer, H. Abdi, A. Azad, J. Bazov, K. N. Chi, P. C. Black and H. Ma, *Lab Chip*, 2015, **15**, 2278-2286.

30. A. F. Sarioglu, N. Aceto, N. Kojic, M. C. Donaldson, M. Zeinali, B. Hamza, A. Engstrom, H. Zhu, T. K. Sundaresan, D. T. Miyamoto, X. Luo, A. Bardia, B. S. Wittner, S. Ramaswamy, T. Shioda, D. T. Ting, S. L. Stott, R. Kapur, S. Maheswaran, D. A. Haber and M. Toner, *Nat Methods*, 2015, **12**, 685-691.

31. E. Sollier, D. E. Go, J. Che, D. R. Gossett, S. O'Byrne, W. M. Weaver, N. Kummer, M. Rettig, J. Goldman, N. Nickols, S. McCloskey, R. P. Kulkarni and D. Di Carlo, *Lab Chip*, 2014, **14**, 63-77.

32. H. W. Hou, M. E. Warkiani, B. L. Khoo, Z. R. Li, R. A. Soo, D. S. Tan, W. T. Lim, J. Han, A. A. Bhagat and C. T. Lim, *Sci Rep*, 2013, **3**, 1259.

33. V. Gupta, I. Jafferji, M. Garza, V. O. Melnikova, D. K. Hasegawa, R. Pethig and D. W. Davis, *Biomicrofluidics*, 2012, **6**, 24133.

34. P. Li, Z. Mao, Z. Peng, L. Zhou, Y. Chen, P. H. Huang, C. I. Truica, J. J. Drabick, W. S. El-Deiry, M. Dao, S. Suresh and T. J. Huang, *Proc Natl Acad Sci U S A*, 2015, **112**, 4970-4975.

35. M. Antfolk, C. Antfolk, H. Lilja, T. Laurell and P. Augustsson, *Lab Chip*, 2015, **15**, 2102-2109.

36. W. Zhao, R. Cheng, B. D. Jenkins, T. Zhu, N. E. Okonkwo, C. E. Jones, M. B. Davis, S. K. Kavuri, Z. Hao, C. Schroeder and L. Mao, *Lab Chip*, 2017, **17**, 3097-3111.